

Phase Coherent Timing of PSR J1811–1925: The Pulsar at the Heart of G11.2–0.3

F.P. Gavriil ¹, V.M. Kaspi ¹, and M.S.E. Roberts^{1,2}

¹*Physics Department, McGill University, Montreal, QC H3A 2T8, Canada*

²*Department of Physics and Center for Space Research, Massachusetts Institute of Technology, Cambridge, MA 02139, USA*

ABSTRACT

The X-ray Pulsar PSR J1811–1925 in the historic supernova remnant G11.2–0.3 has a characteristic age over 10 times the age of the remnant. This likely implies that its current spin period, 65 ms, is close to its birth spin period. Alternatively, the pulsar may have an unusually high braking index. We report here on regular *Rossi X-ray Timing Explorer*/Proportional Counting Array (*RXTE*/PCA) timing observations of the pulsar that were designed to measure its braking index. We provide a preliminary phase-coherent timing solution which includes a significant $\ddot{\nu}$. The braking index we measure is $\gg 3$, likely a result of conventional timing noise. We also report on a preliminary analysis of the pulsar’s unusually hard spectrum: we determine a photon index of $\Gamma = 1.78 \pm 0.74$, for the pulsed component of the spectra, consistent within the uncertainties with previous *ASCA* and *Chandra* observations. The pulsed emission of PSR J1811–1925 is seen beyond 30 keV, and the pulsations remain sinusoidal up to and beyond this energy.

INTRODUCTION

The determination of the ages of pulsars is of crucial importance to neutron star astrophysics. Neutron star population synthesis, birthrate, supernova remnant associations, and even cooling timescales (which serve as probes of the neutron star equation of state), all depend on accurate determinations of pulsar ages. In general, a pulsar’s age is estimated by assuming a spin-down evolution of the form

$$\dot{\nu} \propto \nu^n, \quad (1)$$

where n is known as the *braking index*. It can be determined observationally by measuring $\ddot{\nu}$, since, as is easily shown, $n = \nu \ddot{\nu} / \dot{\nu}^2$. Integrating Equation 1 over the lifetime of the pulsar, assuming a constant braking index, results in the following estimate of the pulsar’s age:

$$\tau = \frac{P}{(n-1)\dot{P}} \left[1 - \left(\frac{P_0}{P} \right)^{n-1} \right], \quad (2)$$

where P_0 is the spin period of the pulsar at birth. It is conventional to assume $n = 3$, appropriate for spin-down due to magnetic dipole radiation, and $P_0 \ll P$ to derive the characteristic age $\tau_c = P/(2\dot{P})$.

Timing noise, stochastic variations in the pulse spin-down (see e.g. Lyne et al., 1996), make accurate determinations of the braking index impossible for the large majority of the over 1300 radio pulsars currently known. The five reliably measured radio pulsar braking indices are in the range 1.4 – 2.9 (Kaspi et al., 1994; Lyne et al., 1996; Lyne et al., 1988; Camilo et al., 2000; Zhang et al., 2001). This clearly signals a significant difference between pulsar electrodynamics and a simple dipole spinning down *in vacuo*. This is of major interest to modelers of pulsar magnetospheres (e.g. Melatos, 1997). But it is also very

important for neutron star astrophysics in general: if the braking indices of all pulsars are $n < 3$, then the characteristic age systematically underestimates the true age.

On the other hand, initial spin periods P_0 that are a non-negligible fraction of the current spin period P lead to a systematic over estimation of the true age. The distribution of initial spin periods is also of intrinsic scientific interest, since it gives clues to the physics of the formation of neutron stars as well as such possibilities as early epochs of rapid spin-down due to gravitational radiation or interactions with fossil disks. However, to infer the initial spin period from Equation 2 requires an independent determination of the true age, such as an associated historical event or a well determined age from an associated supernova remnant. This situation is very rare. The best, and until recently only, example is the Crab pulsar, whose measured braking index and known age results in an inferred $P_0 \sim 19$ ms. There are very few other historical supernovae that might be used. Of course an isolated pulsar's current spin period is an upper limit on the initial spin period, so, for example, $P_0 < 16$ ms can be trivially inferred for PSR J0537–6910 in the LMC (Marshall et al., 1998).

PSR J1811–1925 – The Pulsar at the Heart of G11.2–0.3

G11.2–0.3 is a young supernova remnant plausibly associated with the historical “guest star” witnessed by Chinese astronomers in the year 386 A.D. (Clark and Stephenson, 1977). Radio and X-ray estimates of its age (Green et al., 1988; Vasisht et al., 1996), assuming a type II supernova, support the historical association. A young 65-ms pulsar with spin-down energy $\dot{E} = 6.4 \times 10^{36}$ erg s $^{-1}$ was discovered in X-rays by *ASCA* within G11.2–0.3 (Torii et al., 1997). Recent *Chandra* observations place the pulsar at the precise center of the remnant (Kaspi et al., 2001), making the association of the two unambiguous. Surprisingly, the $\dot{P} = 4.4 \times 10^{-14}$, determined from one observation in 1994 and three observations in 1998, implies a characteristic spin-down age of $\tau_c = 24,000$ yr (Torii et al., 1999), 15 times that inferred from the historical association, the remnant radio surface brightness, and the remnant X-ray spectrum. For this large discrepancy to be resolved, either the braking index $n > 30$, or the initial spin period $P_0 \sim 62$ ms is very near the current spin period. Very recently, a similar P_0 was inferred for the newly discovered pulsar in 3C58/SN1181 (Murray et al., 2002), suggesting that such long initial spin periods may be common. Unfortunately, the number of systems where the initial spin period can be estimated is likely to remain small. Therefore, it is crucial that all alternative explanations for the age discrepancy observed in G11.2–0.3 be fully explored.

OBSERVATIONS

The results presented here were obtained using the Proportional Counter Array (PCA) on board the *Rossi X-ray Timing Explorer (RXTE)*. Our observations consist primarily of ~ 20 ks observations taken on a monthly basis.

Phase Coherent Timing

Deep radio searches have been unable to detect the pulsar (Crawford et al., 1998), and so X-ray monitoring of the source is the only option for timing. The spin-down rate \dot{P} of PSR J1811–1925 was first made by Torii et al. (1999) using *ASCA*, essentially on the basis of periods at just two widely spaced epochs. Here we present a phase-coherent timing solution for the pulsar using regular *RXTE* observations.

In the timing analysis, we included only those events having energies in the 2–30 keV energy range so as to maximize the signal-to-noise ratio of the pulse. Each binned time series was epoch-folded using the best estimate frequency determined initially from either a periodogram or Fourier transform (though later folding was done using the timing ephemeris determined by maintaining phase coherence; see below). Resulting pulse profiles were cross-correlated in the Fourier domain with a high signal-to-noise template created by adding phase-aligned profiles from previous observations. The 2–30 keV template is shown in Figure 1. The cross-correlation returns an average pulse time-of-arrival (TOA) for each observation corresponding to a fixed pulse phase. The pulse phase ϕ at any time t can be expressed as a Taylor expansion,

$$\phi(t) = \phi(t_0) + \nu_0(t - t_0) + \frac{1}{2}\dot{\nu}_0(t - t_0)^2 + \frac{1}{6}\ddot{\nu}_0(t - t_0)^3 + \dots, \quad (3)$$

where $\nu \equiv 1/P$ is the pulse frequency, $\dot{\nu} \equiv d\nu/dt$, etc. and subscript ‘0’ denotes a parameter evaluated at the reference epoch $t = t_0$. The TOAs were fit to the above polynomial using the pulsar timing software package

Parameter	Value
R.A. (J2000)	18 ^h 11 ^m 29 ^s .22
Decl. (J2000)	-19° 25' 27."6
Range of MJDs	52341–52541
No. Pulse Arrival Times	18
ν (Hz)	15.461208393(11)
$\dot{\nu}$ ($\times 10^{-11}$ Hz s ⁻¹)	-1.00975(28)
$\ddot{\nu}$ ($\times 10^{-20}$ Hz s ⁻²)	1.40(3)
P (ms)	64.67799741(44)
\dot{P} ($\times 10^{-15}$ s s ⁻¹)	42.240(12)
Epoch (MJD)	52341.8046
RMS Residual (ms)	2.7
Surface Magnetic Field, B_s ($\times 10^{12}$ G)	1.7
Spin-down Luminosity, \dot{E} ($\times 10^{36}$ erg s ⁻¹)	6.1
Characteristic Age, τ_c (kyr)	24

Table 1. Spin parameters for PSR J1811–1925 derived from phase coherent timing of this source for ~ 9 months.

TEMPO¹. Unambiguous pulse numbering is made possible by obtaining monitoring observations spaced so that the best-fit model parameters have a small enough uncertainty to allow prediction of the phase of the next observation to within ~ 0.2 , this was accomplished by two closely spaced observations (within a few of hours of each other) followed by one spaced a few days later. We are now capable of maintaining phase coherence with regular monitoring observations.

Arrival time residuals for PSR J1811–1925 are shown in Figure 2. Spin parameters determined via phase-coherent timing using nine months of *RXTE* data are presented in Table 1. Phase residuals from the simple model given in Table 1 are random, though not completely consistent with zero given the uncertainties, which are typically ~ 1 ms. This suggests there might be some pulse “jitter,” as is sometimes seen in radio pulsar timing. The tabulated spin parameters include a significant frequency second derivative. These parameters imply a braking index $n = 1980 \pm 93$. This number is much larger than the canonical value of 3. This could reflect highly unusual spin-down behavior, unprecedented in rotation-powered pulsars. If so, the initial spin period would not be determined for this pulsar. A more likely scenario is that the large value measure for n reflects conventional timing noise, common to rotation-powered pulsars. In this case, a future measurement of the true, deterministic value of n is not precluded.

Spectroscopy

This source is of particular interest given its relatively hard spectrum, as, unlike most X-ray detected pulsars, pulsed emission well above 10 keV is definitely detected. We studied the pulsed spectrum by summing all our folded, phase aligned time series into two energy bands (2–10 keV and 10–30 keV). The folded profiles in these energy bands were identical. The 2–30 keV profile is displayed in Figure 1.

In order to obtain a high signal-to-noise pulsed spectrum for PSR J1811–1925, data from each observing epoch were folded at the expected pulse period as was done for the timing analysis. However, here, 8 phase bins were used across the pulse. For each phase bin, we maintained a spectral resolution of 128 bins over the PCA range. One off-pulse phase bin was used as a background estimator. The pulse profiles were then phase aligned, so that the same off-pulse bin was used for background in every case. The remaining phase bins were summed, and their spectral bins regrouped into groups of 4 using the FTOOL `grppha`. Energies below 2 keV and above 70 keV were ignored, leaving 23 spectral channels for fitting. The regrouped, phase-summed data set, along with the background measurement, were used as input to the X-ray spectral fitting

¹<http://pulsar.princeton.edu/tempo>

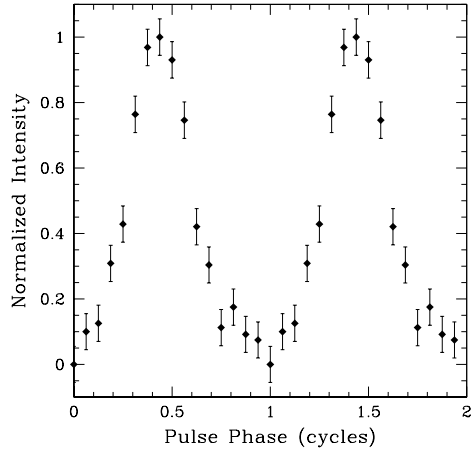


Fig. 1. X-ray pulse profile in the 2–30 keV range. Two cycles are shown for clarity. Profiles in the 2–10 keV and 10–30 keV range are identical.

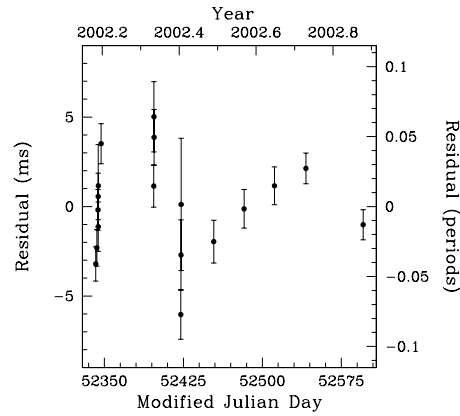


Fig. 2. Post-fit residuals for PSR J1811–1925 after removal of the best-fit spin parameters in Table 1.

Parameter	Value
Γ	1.78 ± 0.74
n_H ($\times 10^{22}$ cm $^{-2}$)	2.36 (fixed)
Flux ($\times 10^{-12}$ erg cm $^{-2}$ s $^{-1}$)	1.18 ± 0.36 (2–10 keV)
L_x ($\times 10^{32}$ erg s $^{-1}$)	2.81 ± 0.86 (2–10 keV)
χ^2_ν (ν)	0.88 (21)

Table 2. Spectral fit of the pulsed component of PSR J1811–1925 to a simple photoelectrically absorbed power-law model of photon index Γ . The errors quoted indicate 90% confidence intervals. The X-ray luminosity L_x , in the 2–30 keV range, was calculated assuming a distance of 5 kpc (Becker et al., 1985; Green, 1998) and assuming a beaming fraction of 1 sr.

software package **XSPEC**². Response matrices were created using the FT00Ls **xtefilt** and **pcarsp**. We fit the data using a simple photoelectrically absorbed power law, holding only N_H fixed at the value found by Roberts et al. (2002) (see Table 2). Uncertainties were measured using the **XSPEC** command **steppar**. The photon index Γ we obtained is consistent within the uncertainties with the value ($\Gamma = 1.11^{+0.37}_{-0.11}$) found by Roberts et al. (2002) using *Chandra* observations.

DISCUSSION

The ratio of the pulsed X-ray luminosity in the 2–10 keV band to \dot{E} gives an efficiency,

$$\eta_x \equiv \frac{L_x}{4\pi I \dot{P} / P^3} = 0.06\%, \quad (4)$$

assuming isotropic emission. Comparing the efficiencies calculated by Possenti et al. (2002) for the 41 known rotation-powered X-ray pulsars, PSR J1811–1925 is the third most efficient, with PSR J1846–0258 (Gotthelf et al., 2000) being the first, and PSR B1509–58 (Cusumano et al., 2001) the second. Note that the efficiencies calculated by Possenti et al. (2002) often included unpulsed contributions resulting from pulsar wind nebular emission, therefore their efficiencies can only be considered upper limits to the pulsed efficiencies. It is interesting to note the similarities among the three most X-ray efficient rotation-powered

²<http://xspec.gsfc.nasa.gov>

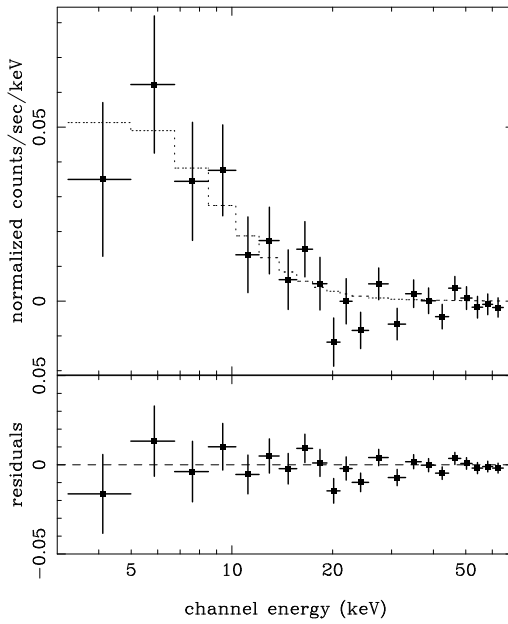


Fig. 3. Top: Phase-averaged spectrum of the pulsed component of PSR J1811–1925. The dash-line indicates a simple photoelectrically absorbed power-law model. Bottom: residuals after subtraction of the model.

pulsars: (i) they all have long duty-cycles, with profiles that remain broad even to high energies (> 10 keV) (ii) they have very hard spectra with photon indices $\Gamma \sim 1.1 - 1.3$ (iii) they are all very young (< 2000 yrs) pulsars in the centers of supernova remnants (iv) they all have pulsar wind nebulae. Furthermore, none of these pulsars have been detected in high energy γ -rays ($E > 100$ MeV). This is in contrast to pulsars such as the Crab, Vela, and PSR B1706–44 (Gotthelf et al., 2002), which have very narrow X-ray pulse profiles, relatively low X-ray efficiencies, but are all detected in high energy γ -rays.

The spectrum and pulse morphology can give us a clue to the emission mechanism at work in PSR J1811–1925. High-energy emission mechanism models generally fall into two classes: polar cap models (e.g. Harding et al., 2002) and outer gap models (e.g. Romani, 2002). The two harder components of the four component X-ray profile (in the *RXTE* band) of the Vela pulsar, which are as hard or harder than PSR J1811–1925 are due to particle curvature emission according to the polar cap model (see Harding et al., 2002). These two components are very narrow and phase aligned with the double peaked γ -ray pulse. For PSR J1811–1925, the broad profile and the absence of γ -ray pulsations make a similar mechanism unlikely. In the outer gap model, the broad, hard profile of PSR J1811–1925 would be from the tail of the synchrotron component. According to Romani (2002), the peak of the synchrotron spectrum for PSR J1811–1925 would occur at $E \sim 31$ MeV, this could be verified with γ -ray observatories such as *GLAST* and *INTEGRAL*.

ACKNOWLEDGMENTS

This work was supported in part by a NASA LTSA grant, an NSERC Research Grant. VMK is a Canada Research Chair. This research has made use of data obtained through the High Energy Astrophysics Science Archive Research Center Online Service, provided by the NASA/Goddard Space Flight Center.

References

- Becker, R. H., Markert, T., and Donahue, M., Radio and X-ray observations of G11.2–0.3 and G41.1–0.3. *ApJ*, **296**, 461–468, 1985.
- Camilo, F. M., Kaspi, V. M., Lyne, A. G., Manchester, R. N., Bell, J. F., D’Amico, N., McKay, N. P. F., and Crawford, F., Discovery of two high-magnetic-field radio pulsars. *ApJ*, **541**, 367–373, 2000.
- Clark, D. H. and Stephenson, F. R., *The Historical Supernovae*. Pergamon, Oxford, 1977.
- Crawford, F., Kaspi, V. M., Manchester, R. N., Camilo, F., Lyne, A. G., and D’Amico, N., Upper limits on

radio emission from the young X-ray pulsars in the supernova remnants G11.2–0.3 and N157B. *Memorie della Societa Astronomica Italiana*, **69**, 951–+, 1998.

Cusumano, G., Mineo, T., Massaro, E., Nicastro, L., Trussoni, E., Massaglia, S., Hermsen, W., and Kuiper, L., The curved X-ray spectrum of PSR B1509–58 observed with *BeppoSAX*. *A&A*, **375**, 397–404, 2001.

Gotthelf, E. V., Halpern, J. P., and Dodson, R., Detection of Pulsed X-Ray Emission from PSR B1706–44. *ApJ*, **567**, L125–L128, 2002.

Gotthelf, E. V., Vasisht, G., Boylan-Kolchin, M., and Torii, K., A 700 year-old pulsar in the supernova remnant Kesteven 75. *ApJ*, **542**, L37–L40, 2000.

Green, D. A., *A Catalogue of Galactic Supernova Remnants (1998 September Version)*. Mullard Radio Astronomy Observatory, Cambridge. (<http://www.mrao.cam.ac.uk/surveys/snrs/>), 1998.

Green, D. A., Gull, S. F., Tan, S. M., and Simon, A. J. B., G11.2–0.3, An evolved Cassiopeia A. *MNRAS*, **231**, 735–738, 1988.

Harding, A. K., Strickman, M. S., Gwinn, C., Dodson, R., Moffet, D., and McCulloch, P., The Multicomponent Nature of the Vela Pulsar Nonthermal X-Ray Spectrum. *ApJ*, **576**, 376–380, 2002.

Kaspi, V. M., Manchester, R. N., Siegman, B., Johnston, S., and Lyne, A. G., On the spin-down of PSR B1509–58. *ApJ*, **422**, L83–L86, 1994.

Kaspi, V. M., Roberts, M. E., Vasisht, G., Gotthelf, E. V., Pivovaroff, M., and Kawai, N., *Chandra* X-Ray Observations of G11.2–0.3: Implications for Pulsar Ages. *ApJ*, **560**, 371–377, 2001.

Lyne, A. G., Pritchard, R. S., and Smith, F. G., Crab pulsar timing 1982–1987. *MNRAS*, **233**, 667–676, 1988.

Lyne, A. G., Pritchard, R. S., Smith, F. G., and Camilo, F., Very low braking index for the Vela pulsar. *Nature*, **381**, 497–498, 1996.

Marshall, F. E., Gotthelf, E. V., Zhang, W., Middleditch, J., and Wang, Q. D., Discovery of an ultra-fast X-ray pulsar in the supernova remnant N157B. *ApJ*, **499**, L179–L182, 1998.

Melatos, A., Spin-down of an oblique rotator with a current starved outer magnetosphere. *MNRAS*, **288**, 1049–1059, 1997.

Murray, S. S., Slane, P. O., Seward, F. D., Ransom, S. M., and Gaensler, B. M., Discovery of X-Ray Pulsations from the Compact Central Source in the Supernova Remnant 3C 58. *ApJ*, **568**, 226–231, 2002.

Possenti, A., Cerutti, R., Colpi, M., and Mereghetti, S., Re-examining the X-ray versus spin-down luminosity correlation of rotation powered pulsars. *A&A*, **387**, 993–1002, 2002.

Roberts, M. S. E., Tam, R. C., Kaspi, V. M., Lyutikov, M., Vasisht, G., Pivovaroff, M., Gotthelf, E. V., and Kawai, N., The Pulsar Wind Nebula in G11.2–0.3. *ApJ*. submitted, 2002.

Romani, R. W., The Rest of the Story: Radio Pulsars and IR through Gamma-Ray Emission. to appear in proceedings of the conference “Radio Pulsars” held in Chania, Crete, Sept 2002.

Torii, K., Tsunemi, H., Dotani, T., and Mitsuda, K., Discovery of a 65 ms pulsar in the supernova remnant G11.2–0.3 with *ASCA*. *ApJ*, **489**, 145, 1997.

Torii, K., Tsunemi, H., Dotani, T., Mitsuda, K., Kawai, N., Kinugasa, K., Saito, Y., and Shibata, S., Spin-down of the 65 ms pulsar in the supernova remnant G11.2–0.3. *ApJ*, **523**, 69, 1999.

Vasisht, G., Aoki, T., Dotani, T., Kulkarni, S. R., and Nagase, F., Detection of a hard X-ray plerion in the candidate historical remnant G11.2–0.3. *ApJ*, **456**, 59, 1996.

Zhang, W., Marshall, F. E., Gotthelf, E. V., Middleditch, J., and Wang, Q. D., A Phase-connected Braking Index Measurement for the Large Magellanic Cloud Pulsar PSR B0540–69. *ApJ*, **554**, L177–L180, 2001.